bioRxiv preprint doi: https://doi.org/10.1101/604660; this version posted April 10, 2019. The copyright holder for this preprint (which was not certified by peer review) is the author/funder, who has granted bioRxiv a license to display the preprint in perpetuity. It is made available under aCC-BY-NC-ND 4.0 International license.

Yeast Sup35 prion structure: two types, four parts, many variants

Alexander A. Dergalev, Alexander I. Alexandrov, Roman I. Ivannikov, Michael D. Ter-Avanesyan and Vitaly V. Kushnirov*

Research Center of Biotechnology of Russian Academy of Sciences, A.N. Bach Institute of Biochemistry, Moscow, Russia

*Corresponding author

E-mail: vvkushnirov@gmail.com

bioRxiv preprint doi: https://doi.org/10.1101/604660; this version posted April 10, 2019. The copyright holder for this preprint (which was not certified by peer review) is the author/funder, who has granted bioRxiv a license to display the preprint in perpetuity. It is made available under aCC-BY-NC-ND 4.0 International license.

Abstract

The yeast [*PSI*$^+$] prion, formed by the Sup35 (eRF3) protein, can exist as multiple structural variants exhibiting phenotypic variation in the strength of nonsense suppression and mitotic stability. Structure of [*PSI*$^+$] and its variation is only partly characterized. Here, we mapped the Sup35 proteinase K-resistant amyloid cores of 26 [*PSI*$^+$] prions of different origin, isolated from yeast cells. In all cases the Sup35 amino acid residues 2-32 were fully resistant and the region up to residue 72 was partially resistant. Proteinase K-resistant structures were also found within regions 73-124, 125-153 and 154-221, but their presence differed between [*PSI*$^+$] isolates. The [*PSI*$^+$] phenotype depended mainly, if not solely, on the structure in region 2-72. Structures in region 73-221 were in some cases mitotically unstable and heterogenous. Two distinct digestion patterns were observed for the 2-72 fragment, which correlated with the "strong" and "weak" [*PSI*$^+$] nonsense-suppressor phenotypes. All [*PSI*$^+$] with a weak pattern were eliminated by multicopy *HSP104* gene and were not toxic when combined with multicopy *SUP35*. [*PSI*$^+$] with a strong pattern showed opposite properties, being resistant to multicopy *HSP104* and lethal in the presence of multicopy *SUP35*. Thus, our data suggest existence of two distinct and reliably distinguishable structural classes of [*PSI*$^+$] rather than a continuum of prions with gradually altering phenotype.

bioRxiv preprint doi: https://doi.org/10.1101/604660; this version posted April 10, 2019. The copyright holder for this preprint (which was not certified by peer review) is the author/funder, who has granted bioRxiv a license to display the preprint in perpetuity. It is made available under aCC-BY-NC-ND 4.0 International license.

Importance

Prions and amyloids are relatively novel and incompletely characterized structures. To understand them better, we mapped amyloid cores of 26 isolates of the Sup35 yeast prion using proteinase K digestion and mass spectrometry. We found that these cores are composed of up to four proteinase K-resistant elements spanning almost the whole length of Sup35 region inessential for viability. However, only the N-terminal element was present in all structures. There are many variants of the Sup35 prion, and these are usually roughly combined into two groups, "strong" and "weak", based on the strength of their nonsense-suppressor phenotype. However, it was not clear whether such groups could be distinguished by any reliable qualitative criteria. Our data indicate that these groups do exist and can be reliably distinguished based on the N-terminal element digestion pattern and the effects of the multicopy *SUP35* and *HSP104* genes on these prion variants.

Keywords: prion; amyloid; prion variants; prion core; proteinase K; Sup35; Rnq1

bioRxiv preprint doi: https://doi.org/10.1101/604660; this version posted April 10, 2019. The copyright holder for this preprint (which was not certified by peer review) is the author/funder, who has granted bioRxiv a license to display the preprint in perpetuity. It is made available under aCC-BY-NC-ND 4.0 International license.

Introduction

With few exceptions, prions represent an infectious variety of amyloids. Amyloids are fibers composed of many molecules of the same protein (protomers), whose altered conformation is reproduced along the fiber. Thus, amyloids can be considered as one-dimensional crystals, in contrast to more common 3D crystals. In amyloid fibers, polypeptide chains are perpendicular to the fiber axis and form multimolecular beta sheets, which are parallel to the axis. However, finer details of amyloid structure are poorly characterized. In many cases, and in particular in yeast prions, amyloids follow two novel and unprecedented structural principles: each protomer forms a single 4.7Å layer along the fiber axis, and neighboring polypeptide chains are located parallel and in-register (1, 2). Usually only a part of a protomer adopts amyloid structure and forms a stem of amyloid, while the rest of protomer is loosely attached to this stem (3) and can even retain its original structure and function (4). Such division is especially clear in yeast prionogenic proteins, which contain separate functional and aggregation domains.

In yeast, prions manifest themselves as heritable genetic elements. The best studied of yeast prions is [*PSI*$^+$], formed by the prion form of the essential translation termination factor eRF3, also known as Sup35. Sup35 is composed of three domains (5, 6). The N-terminal (N) domain (amino acid residues 1-123) is necessary and sufficient for the [*PSI*$^+$] propagation. The middle (M) domain (residues 124-253) interacts with the Hsp104 chaperone through the region 128-148, and is also involved in the liquid-liquid phase separation behavior of Sup35 (7, 8). The essential C-terminal domain (residues 254-685) acts in translation termination (6).

A single protein can form amyloids with different structures. In the case of yeast Sup35 protein these structures manifest as [*PSI*$^+$] variants differing in nonsense suppression and mitotic stability (9). The relation between prion phenotype and amyloid structure is mediated, in particular, by quantitatively different activity of the Hsp104 chaperone, assisted by the Hsp70 and Hsp40 chaperones, towards different prions (10). Hsp104 severs Sup35 amyloids into smaller pieces, thus multiplying amyloid ends, which can engage new Sup35 molecules into amyloid (11, 12). The

bioRxiv preprint doi: https://doi.org/10.1101/604660; this version posted April 10, 2019. The copyright holder for this preprint (which was not certified by peer review) is the author/funder, who has granted bioRxiv a license to display the preprint in perpetuity. It is made available under aCC-BY-NC-ND 4.0 International license.

amyloid structure defines how frequently it is recognized by Hsp104 and/or how easily Hsp104 can extract a protomer, thus cleaving an amyloid particle in two pieces. More frequent cleavage usually results in smaller, but more numerous, amyloid particles, faster amyloid conversion, lower levels of non-aggregated functional Sup35, higher suppression and more stable inheritance (10). Such [*PSI*$^+$] are called "strong". Less frequent Hsp104 action results in "weak" [*PSI*$^+$], distinguished by moderate suppression and higher levels of non-aggregated Sup35. The actual number of alternative Sup35 amyloid structures, manifested as [*PSI*$^+$] variants, is unclear and can be very high, but usually not more than four [*PSI*$^+$] variants can be reliably distinguished by nonsense suppression (13) or other phenotypes (14–16). It is also unclear whether all [*PSI*$^+$] variants can be divided into two distinct groups, such as strong and weak, or they represent a continuum with gradually altering phenotype. Most studies tested only one representative of each type, which did not allow addressing this question. However, measurement of nonsense readthrough in 51 fresh [*PSI*$^+$] isolates (17) indicated in favor of the latter opportunity.

The Sup35 prion structure was studied in several works, but it is still far from being fully understood and the proposed structures are somewhat contradictory (18–20).

A powerful, though rarely used approach for such studies is mapping of areas resistant to digestion with proteinase K (PK) (termed the prion core) using mass spectrometric identification of digestion-resistant peptides. Previous studies of the Sup35 prion structure with PK used Sup35NM amyloids obtained *in vitro* at either 4 or 37ºC, which mainly produce, respectively, strong and weak [*PSI*$^+$], when introduced into yeast cells. However, it is unclear, how faithfully such amyloids recapitulate the properties of prions existing *in vivo*. In particular, such amyloids are to a certain extent heterogeneous (21) and this is difficult to control.

Here, we developed a set of methods to isolate prions from yeast cells with sufficient quality and analyze their structure using PK digestion. This allowed construction of precise maps of the Sup35 prion core of many [*PSI*$^+$] variants, providing details of molecular structure. Strikingly, our results differed considerably from those obtained with *in vitro* fibrils.

bioRxiv preprint doi: https://doi.org/10.1101/604660; this version posted April 10, 2019. The copyright holder for this preprint (which was not certified by peer review) is the author/funder, who has granted bioRxiv a license to display the preprint in perpetuity. It is made available under aCC-BY-NC-ND 4.0 International license.

Results

General structure of Sup35 prion. To characterize the Sup35 amyloid structures in different [*PSI*$^+$] variants, we mapped the Sup35 regions resistant to PK, which likely correspond to amyloid core regions. PK-resistant peptides were identified by MALDI-TOF. The studied [*PSI*$^+$] variants were existing and new isolates obtained in yeast strains 5V-H19 and 74-D694 in standard and non-standard ways (Table 1). For clarity, all [*PSI*$^+$] isolates were named so that the first letter indicated the [*PSI*$^+$] type, as defined in this work: S, strong, or W, weak.

Sup35 prions were isolated from yeast cells overproducing Sup35 N and M domains (residues 1-239) fused to hexahistidine and GFP (Sup35NMG) under control of a *GAL1* promoter, and encoded on a multicopy plasmid. The Sup35 prion samples were isolated and digested with PK in the presence of 0.5% Sarcosyl. This ionic detergent does not inhibit PK activity and does not disassemble amyloid fibers. Notably, in contrast to earlier reports that PK cuts proteins after aliphatic and hydrophobic residues (22) and public databases (https://web.expasy.org/peptide_cutter/), we did not observe any significant residue specificity. Almost all types of amino acid residues were found at the C-termini of identified Sup35 fragments, except for proline.

As predicted (23), the N-terminal methionine of Sup35 was fully removed and replaced with an acetyl group.

PK-resistant peptides were found along the whole length of the Sup35 N and M domains, up to residue 221. Their location was not random: in all [*PSI*$^+$] variants they were enclosed within regions 1-72, 73-124, 125-153 and 154-221, termed Regions 1, 2, 3 and 4 in this work (Fig. 1). The corresponding PK-resistant structures in these regions were denoted as Cores 1, 2, 3 and 4. A small exception was a rarely observed group of fragments spanning Regions 2 and 3. Core 1 was present in all [*PSI*$^+$] isolates, while the presence of Cores 2 to 4 varied. Region 222-233 was never protected

bioRxiv preprint doi: https://doi.org/10.1101/604660; this version posted April 10, 2019. The copyright holder for this preprint (which was not certified by peer review) is the author/funder, who has granted bioRxiv a license to display the preprint in perpetuity. It is made available under aCC-BY-NC-ND 4.0 International license.

from PK. The remaining Sup35 region 234-239 was often found as a part of PK-resistant peptides, but the other part of all of these peptides represented sequences unrelated to Sup35, such as hexahistidine and GFP, and so these peptides were ignored.

No PK-protected fragments of Sup35NM were observed, when Sup35NMG (preparations W-T7, S-W8R41, S-VH0) was boiled prior to PK digestion, which should dissolve all structures. This indicated that PK fully digested unstructured Sup35NM, and so all Sup35NM PK-resistant fragments observed in [*PSI*$^{+}$] preparations reflected structures within Sup35.

PK digestion of soluble Sup35NMG isolated from 74-D694 [*psi*$^{-}$] Δ*rnq1* cells using hexahistidine tag revealed no peptides from Regions 1-3 and only a minor amount of peptides belonging to Region 4. Thus, soluble Sup35NM lacks PK-resistant structure, except for a small fraction of molecules structured in the Region 4.

In earlier works, the MS analysis of PK digestion was represented by simply showing MS spectra (21, 24). However, in this work such an approach was convenient only to represent digestion of Core 1, but not the whole Sup35NM profile, because the number of identified PK-resistant peptides was significantly higher than in previous works, about 30 to 60 peptides in each preparation, and often the peptides from different regions of Sup35NM were located in close proximity on an MS spectrum. For convenient presentation of these data, we developed a novel procedure. We summed up these peptides accounting to their apparent abundance as follows. For every residue of Sup35NM, we calculated the PK resistance index (R) as a sum of MS peak areas of PK resistant peptides which include this residue. This index was normalized against its maximum value for each preparation, so that each graph would fit in the range of 0 to 1 (Fig. 2A and S1).

Though MALDI is not regarded as a quantitative procedure, the obtained profiles were sufficiently reproducible. In particular, the profiles were very similar between weak [*PSI*$^{+}$] variant W-1112 and its derivatives, and similar to W-Pb and W-HT2889 (Fig. S1-25, 27, 29-31). For W-1112 we also tested whether PK resistance profile depends on Sup35NMG production level. Prion fractions were isolated from W-1112 cells without Sup35NMG production and with moderate

bioRxiv preprint doi: https://doi.org/10.1101/604660; this version posted April 10, 2019. The copyright holder for this preprint (which was not certified by peer review) is the author/funder, who has granted bioRxiv a license to display the preprint in perpetuity. It is made available under aCC-BY-NC-ND 4.0 International license.

154 overproduction from single-copy *GAL1* promoter. The obtained profiles were similar to the one
155 obtained with high Sup35NMG overproduction from multicopy *GAL1* promoter (Fig. 1A). This
156 indicates that high overproduction did not significantly alter prion structure. However, analysis of
157 preparations with no or low Sup35NMG overproduction was complicated by high background and
158 presence of peptides unrelated to Sup35. For this reason, we used high Sup35NMG overproduction
159 in this study.

160

161 **C-terminal core of the Rnq1 prion.** Two peptides, frequently found in Sup35NMG PK digests
162 were identified as the Rnq1 fragments 366-405 and 360-405 (Fig. S1). Ten more Rnq1 fragments
163 were minor and found mostly in preparations where Sup35 was not overproduced. In mirror
164 similarity to the Sup35 Core 1, all these fragments ended at the C-terminus. The size of Rnq1
165 peptides was from 26 to 50 residues. No Rnq1 peptides were observed in preparations from [*pin*$^-$]
166 and *Δrnq1* cells.

167

168 **Weak and strong [*PSI*$^+$] differ in Core 1 structure.** While the major visual difference between
169 [*PSI*$^+$] isolates was the presence or absence of Cores 2, 3 and 4, the strength of the [*PSI*$^+$] phenotype
170 correlated with less prominent differences in the structure of Core 1, which are better seen on MS
171 spectra (Fig. 2B and S1). We observed two major patterns of Core 1 digestion, which fully
172 correlated with our initial assignment of [*PSI*$^+$] variants as weak or strong basing on colony color
173 and nonsense codon readthrough (Fig. 3).

174 In all studied samples the N-terminal region of about 31 residues was fully protected from PK
175 digestion. This region spanned residues 2-32 in weak variants, and 2-32 or 2-30 in strong ones, but
176 the 2-30 peptide was minor and thus poorly accessible. Partial protection from PK usually extended
177 over a larger area, up to residue 72.

178 In the strong [*PSI*$^+$] variants the most abundant PK-resistant peptides were 2-35 and 2-38, while
179 in weak variants these were 2-42 and 2-45. Another significant difference was that the region 42-72

bioRxiv preprint doi: https://doi.org/10.1101/604660; this version posted April 10, 2019. The copyright holder for this preprint (which was not certified by peer review) is the author/funder, who has granted bioRxiv a license to display the preprint in perpetuity. It is made available under aCC-BY-NC-ND 4.0 International license.

was much better protected in strong [*PSI*$^+$] variants, in which we observed less peptides ending in this region. As a result, a group of peptides 2-70, 2-71 and 2-72 was often the most abundant in strong [*PSI*$^+$] preparations, while in weak [*PSI*$^+$] it was minor or almost absent. The variant S-W8 was unique among strong [*PSI*$^+$], since, in addition to characteristic peptides 2-35 and 2-38, it showed a major resistant peptide 2-57 instead of 2-70, thus somewhat resembling weak variants (Fig. 2B and S1-17).

Interestingly, the PK resistance of region 33-72 depended on its connection to the fully protected core 2-32. Of all possible internal peptides of the region 33-72, we observed only trace amounts of peptides 38-70 and 38-71, and only in some strong [*PSI*$^+$] preparations. This shows that the region 33-72 becomes highly sensitive to PK after being cleaved from the fully protected 2-32 core.

Core 2 usually occupied region 91-120 in weak [*PSI*$^+$] and 81-100 in strong [*PSI*$^+$] (Table 2). In weak isolates Core 2 was found more frequently and showed higher PK resistance. In S-W8 variant Core 2 was intermediate between the weak and strong types and occupied the region 91-113. Core 3 usually spanned the region 125-148 and was more frequent in strong [*PSI*$^+$] isolates (Table 2). Cores 2 and 3 were less PK-resistant than Core 1 and their visible proportion decreased at higher levels of PK.

Additional phenotypical assays distinguishing weak and strong [*PSI*$^+$] types. Since our PK digestion data suggested that various types of [*PSI*$^+$] belonged to two distinct structural classes, and did not represent a continuum of structural variants, we looked whether their difference could be observed as clearly in other assays. Earlier we and others observed that strong and weak [*PSI*$^+$] react differently to overexpression of the *SUP35* and *HSP104* genes. Strong [*PSI*$^+$] was extremely toxic or lethal in combination with multicopy *SUP35* (25) and was not cured by multicopy *HSP104* (12). Weak [*PSI*$^+$] variants showed opposite behavior, being nontoxic with multicopy *SUP35* (25) and very sensitive to multicopy *HSP104* (14, 26). However, the earlier studies tested single

bioRxiv preprint doi: https://doi.org/10.1101/604660; this version posted April 10, 2019. The copyright holder for this preprint (which was not certified by peer review) is the author/funder, who has granted bioRxiv a license to display the preprint in perpetuity. It is made available under aCC-BY-NC-ND 4.0 International license.

206 representatives of strong and weak [*PSI*$^+$], and so it was not clear, how general these observations
207 are.

208 We transformed 15 [*PSI*$^+$] variants with multicopy plasmids with the *HSP104*, *SUP35* as well as
209 *SUP35NM* genes (Fig. 4). Multicopy *HSP104* eliminated all weak [*PSI*$^+$], and did not eliminate
210 strong ones. Multicopy *SUP35* was highly toxic for S-VH and S-W8, and lethal for other strong
211 [*PSI*$^+$]; it was slightly toxic for S-L2 and non-toxic for other weak [*PSI*$^+$]. The effect of excess
212 Sup35 on strong [*PSI*$^+$] cells was so dramatic that even low copy centromeric *SUP35* (presumably,
213 single-copy due to negative selection) caused significant retardation of growth of the S1 [*PSI*$^+$] (Fig.
214 4). Thus, all variants showed either one of the two described opposite modes of behavior in strict
215 dependence on structure of the Core 1. Even the variant S-W8, which showed some structural
216 similarity with weak [*PSI*$^+$] and the nonsense readthrough level intermediate between strong and
217 weak variants, was unambiguously classified as strong. Therefore, strong and weak [*PSI*$^+$] variants
218 represent two distinct classes, which are readily distinguished by the structure of Core 1 and by the
219 effects of multicopy *SUP35* and *HSP104* genes.

220 The lethality of strong [*PSI*$^+$] combined with multicopy *SUP35* was relieved, when *SUP35* was
221 supplemented with an equal number of copies of the *SUP45* gene. This confirms earlier reports that
222 the lethality is related to depletion of the essential translation termination factor Sup45 (eRF1) (25).
223 Moreover, multicopy *SUP45* caused a significant antisuppressor effect, as observed earlier (27).
224 Multicopy *SUP35NMG* was less toxic than *SUP35*. This agrees with the Sup45 depletion model,
225 since Sup35NMG lacks the Sup35 C domain, which binds Sup45.

226 Our data on [*PSI*$^+$] curing by *HSP104* overproduction driven by its endogenous promoter may
227 appear to contradict earlier observations that low copy *HSP104* under strong inducible *GAL1*
228 promoter cured strong [*PSI*$^+$] with intermediate efficiency (9, 26). To resolve this contradiction, we
229 transformed cells bearing S1 and S-7 variants with multicopy *HSP104* under its endogenous
230 promoter and plated cells to SC-glucose and SC-galactose media. Transformants were streaked to
231 single cells on YPD-red medium. No red [*psi*$^-$] colonies were observed after SC-glucose, while

bioRxiv preprint doi: https://doi.org/10.1101/604660; this version posted April 10, 2019. The copyright holder for this preprint (which was not certified by peer review) is the author/funder, who has granted bioRxiv a license to display the preprint in perpetuity. It is made available under aCC-BY-NC-ND 4.0 International license.

these constituted about 20% of colonies after SC-galactose (Fig. S2). Thus, [*PSI*$^+$] curing by Hsp104 overproduction depends on carbon source, which resolves the contradiction.

Manipulations with Core 2. To assess whether Core 2 could be selectively eliminated and whether this would affect the nonsense suppressor phenotype, we overproduced the Sup35 deletion variant Sup35(Δ84-112)NMG, lacking a part of Region 2 in [*PSI*$^+$] variants S1, S-W8 and W-1112. We reasoned that the truncated Sup35 should efficiently incorporate into Sup35 prion polymers via Core 1 (13, 15, 28), but would not template Core 2, which should then be eliminated. Then the plasmid encoding Sup35(Δ84-112)NMG was lost, Sup35NMG was overproduced and prion structures were analyzed by PK. Core 2 disappeared in variant S1, but stayed unchanged in W-1112 (Fig. 5A). In S-W8 Core 2 remained, but was altered and Core 3 appeared in one of two cases (Fig. 5A). This allows thinking that Core 1 can predetermine the formation and restoration of Core 2, though not in all cases.

To further characterize the dependence of Core 2 on Core 1, we inserted an additional copy of oligopeptide Repeats 4 and 5 between Regions 1 and 2 without altering these Regions. This protein, Sup35(N+2R)MG, was overproduced in variants W-1112 and S-W8, and its structure was analyzed. Core 2 was essentially unchanged in both variants (Fig. 5B). Thus, in some contrast with the previous observation, Core 2 can propagate relatively independently from Core 1. The distance between Cores 1 and 2 was not critical for Core 2 formation, which suggests that the PK-sensitive region between Cores 1 and 2 is poorly structured or unstructured.

Notably, loss of Core 2 in the S1 variant did not cause a statistically significant change of nonsense readthrough (Fig. 3). In earlier experiments (13) we observed that shuffling of Sup35 for Sup35(Δ84-112) and back did not change phenotype of both strong and weak variants. This suggests that such procedure either did not change Core 2 or Core 2 did not affect phenotype.

bioRxiv preprint doi: https://doi.org/10.1101/604660; this version posted April 10, 2019. The copyright holder for this preprint (which was not certified by peer review) is the author/funder, who has granted bioRxiv a license to display the preprint in perpetuity. It is made available under aCC-BY-NC-ND 4.0 International license.

Instability and heterogeneity of [*PSI*$^+$] variants. While some [*PSI*$^+$] variants resisted directed attempts to eliminate Core 2, in some others Cores 2 and 3 were unstable and could change spontaneously during propagation. We noted that in one of the transformants of S-7 variant with pYes2-Sup35NMG overproduction of Sup35NMG results in a significant proportion of elongated cells, which could indicate defects of cytoskeleton related to insufficient function of Sup35 or Sup45 (29). This prompted us to compare structures of Sup35NMG isolated from this (S-7-3) and two other transformants (S-7 and S-7-4) with standard cell morphology. All three structures differed in either Core 2 or Core3. Isolate S-7-3 was distinguished by the presence of Core 3 (Fig. S1-4). However, it is not certain that this difference is related to phenotype. Also of note, all three transformants did not noticeably differ by colony color despite the differences in Cores 2 and 3 (Fig. S3).

Some preparations, e.g. S1, S-R4b and W-T7 appeared to represent a mix of two types of Core 2, while S-L20 combined Core 2 and Core 2-3 (Fig. S1-1, 10, 24, 8). This probably indicates heterogeneity and instability of Core 2 in these variants. Another issue is that many preparations contained relatively small amounts of resistant peptides from Regions 2, 3 and 4. This could be due to two reasons: either these structures have low resistance to PK, or these structures are present only in a small proportion of molecules.

Involvement of the PK-protected regions in intermolecular structure. All Sup35NMG preparations isolated from [*PSI*$^+$] cells contained amyloid structure, since they all were insoluble in sarcosyl and bound thioflavin T (data not shown). However, this does not mean that all Sup35NM PK-resistant Cores were involved in amyloid intermolecular interactions.

The amyloidogenic potential of Regions 1 and 2 is usually not questioned. Both Regions alone can form amyloid fibers *in vitro*, and these can transform yeast cells to the [*PSI*$^+$] state (15, 30). In line with this, we observed *in vivo* Sup35 amyloids, in which the only PK-resistant core resided in either Region 1 or Region 2. The former were found in several [*PSI*$^+$] variants, in particular, in S-

bioRxiv preprint doi: https://doi.org/10.1101/604660; this version posted April 10, 2019. The copyright holder for this preprint (which was not certified by peer review) is the author/funder, who has granted bioRxiv a license to display the preprint in perpetuity. It is made available under aCC-BY-NC-ND 4.0 International license.

283 L6, S-Cl2, W2 and W-VL (Fig. S1-7, 13, 21, 33). The latter was obtained by overproduction of the
284 Sup35NMG protein lacking the first 30 residues in the 74-D694 [*PIN*$^+$] cells. This protein formed
285 amyloid, though with decreased efficiency, and the only PK-protected region in this amyloid
286 included residues 81 to 113 (Fig. S1-34, Table 2). This allows assuming that Regions 1 and 2 are
287 involved in the amyloid core in all cases when they are protected from PK.

288 The nature of Cores 3 and 4 is less certain. Recently, Sup35 amyloid was obtained *in vitro*, in
289 which the only PK-resistant core spanned region 81-148 and thus included Regions 2 and 3 (24).
290 However, amyloid structures based solely on Region 3 were never shown. The same is true for
291 Region 4, which, besides, contains 52% of charged residues and thus appears unlikely to form
292 amyloid. Our experiments (Supplementary data) indicate in favor of intermolecular amyloid
293 structure of Regions 1 to 3, but leave uncertainty about Region 4. However, more reliable data may
294 be required for the final answer.

295

296 # Discussion

297 **General properties of the Sup35 prion core.** The aim of this work was to establish through PK
298 digestion the structure of Sup35 prion core, its possible variations and their relation to phenotype.
299 We found that the Sup35 prion core is composed of up to four PK-resistant elements, located within
300 Regions 1 (residues 2-72), 2 (73-124), 3 (125-153), and 4 (154-221). Curiously, the border between
301 the Regions 2 and 3 coincided well with that of the N and M domains. The N-terminal Core 1 was
302 present in all preparations, while other Cores differed between variants (Fig. S1). Core 1 was also
303 the largest of these structures and best protected from PK.

304 Core 1 mainly defined the [*PSI*$^+$] phenotype, and so formation of Cores 2 to 4 was expected to
305 have little effect on phenotype. For Core 2 this was confirmed in the case of S1 variant. Region 3
306 roughly corresponds to the sequence 129-148 involved in interaction with Hsp104. Deletion of this
307 sequence changes colony color from white to pink (7), which resembles the difference between
308 weak and strong [*PSI*$^+$]. However, we observed that the difference in Core 3 did not affect colony

bioRxiv preprint doi: https://doi.org/10.1101/604660; this version posted April 10, 2019. The copyright holder for this preprint (which was not certified by peer review) is the author/funder, who has granted bioRxiv a license to display the preprint in perpetuity. It is made available under aCC-BY-NC-ND 4.0 International license.

color in derivatives of variant S7 (Fig. S3). Thus, formation of Core 3 has little, if any, effect on interaction with Hsp104.

Core 2 in variants W-1112 and S-W8 was highly stable and resisted attempts to remove it through transient overproduction of Sup35NMG with deletion overlapping with Core 2, or by insertion of two additional oligopeptide repeats between Cores 1 and 2. In contrast to this, in S-7 Cores 2 and 3 could change spontaneously. In variants S1, S-R4b and W-T7 the PK-resistant peptides from Region 2 appeared to represent two overlapping cores, one of which was typical of strong, and one of weak [*PSI*$^+$] (Fig. S1-1, 10, 24). It also appears likely that low levels of PK-resistant peptides from Regions 2 and/or 3 in some variants are due to presence of Cores 2 and/or 3 in only a fraction of prion particles. Structural heterogeneity of Sup35 prion was observed earlier as "a cloud of variants" (31). Also, electron microscopy of Sup35 preparations seeded *in vitro* by strong or weak [*PSI*$^+$] lysates revealed that two types of Sup35NM fibrils, "thick" and "thin", were simultaneously present in each preparation. In the thick fibrils all Sup35NM was folded, including the M domain, while in the thin fibrils a region approximately corresponding to M domain was unfolded (32).

Our data support the amyloid nature of the Cores 1, 2 and 3, while the nature of Core 4 is questionable. While Region 4 contains a high number of positively and negatively charged residues and thus does not appear amyloidogenic, some earlier studies indirectly support the amyloid nature of Core 4. In the latter cited work (32) the folded state of the M domain was faithfully propagated along fibrils. It seems unlikely that such transmission could occur without formation of intermolecular amyloid structure. Another work showed that of seven leucine residues in the M domain at least five form in-register contact with another Sup35 molecule (2). Since three of these leucines are located in Region 3, and four in Region 4, this indicates that both Cores 3 and 4 form intermolecular in-register contacts.

Two types of [*PSI*$^+$]. [*PSI*$^+$] variants are usually distinguished based on a quantitative parameter, the nonsense codon readthrough, and associated phenotypes such as colony color or growth rate on

bioRxiv preprint doi: https://doi.org/10.1101/604660; this version posted April 10, 2019. The copyright holder for this preprint (which was not certified by peer review) is the author/funder, who has granted bioRxiv a license to display the preprint in perpetuity. It is made available under aCC-BY-NC-ND 4.0 International license.

adenine omission media. By these properties, the variants are usually labeled as weak or strong, although there are more than just two observable grades of phenotype and it was not clear, whether all [*PSI*$^+$] variants can be divided into two or more clearly distinguishable groups by phenotype and/or structure. Here, we established that indeed all studied [*PSI*$^+$] variants can be divided into two reliably distinguishable groups, which can be called weak and strong [*PSI*$^+$], and provided three qualitative criteria to distinguish them: PK digestion pattern of the Core 1 and reaction to the multicopy *SUP35* and *HSP104* genes. The mechanistic basis for the difference of two [*PSI*$^+$] types remains to be established. As a likely possibility, it can be related to different modes of interaction of weak and strong Sup35 prions with chaperones.

We tried to widen the variety of Sup35 prion structures by using non-standard conditions for [*PSI*$^+$] induction. S-Cl prions were obtained at 4ºC in the *Δrnq1* background; Pb and R4b variants were obtained using as inducer altered Sup35NMG proteins with insertion of 29 residues before the Region 1, or deletion of 29 residues from Region 2. Some [*PSI*$^+$] were obtained through the stage of lethal prions similar to those observed by McGlinchey and coauthors (33). However, all [*PSI*$^+$], obtained in unusual ways, showed properties typical of either strong or weak [*PSI*$^+$] types. This suggests that the Sup35 prion structures not belonging to the two described [*PSI*$^+$] types are either rare or do not exist.

Comparison of the Sup35 fibrils obtained *in vitro* and *in vivo*. Many previous studies used as a model of the Sup35 prion structure the Sup35NM amyloids spontaneously formed *in vitro* at 4ºC or at 37ºC, which are regarded as analogs of the strong and weak prion folds, respectively. PK digestion based mapping of such Sup35 amyloids was performed only recently (24), and some results were very different from ours. These authors observed that the major PK-protected peptides in the "strong" fibrils assembled at 4ºC were 2-38, -42, -45, -46; and 2-72 in the "weak" 37ºC assembly. This result is directly opposite to our observations based on 26 prions that the former pattern is typical of weak [*PSI*$^+$], and the latter – of the strong ones. (Fig. 2, S1). Another difference

bioRxiv preprint doi: https://doi.org/10.1101/604660; this version posted April 10, 2019. The copyright holder for this preprint (which was not certified by peer review) is the author/funder, who has granted bioRxiv a license to display the preprint in perpetuity. It is made available under aCC-BY-NC-ND 4.0 International license.

362 is that simultaneous presence of two or more of PK-resistant cores was not observed in the *in vitro*
363 fibrils.

364 The same work described Sup35 amyloids, whose PK-resistant core did not include the N-
365 terminal region, being located between residues 62 or 81 and 144 (24). We observed similar PK-
366 resistant fragments 81, 91-144, but failed to find prions lacking Core 1, and it is doubtful whether
367 such amyloids can propagate as prions *in vivo* for the following reasons. Such amyloids were
368 formed by mutant protein Sup35NM(S17R), and their fold was transferable *in vitro* to wild type
369 Sup35NM. The S17R mutation impairs Core 1 formation, and so do two Sup35 N-terminal
370 deletions, which we tested. The Sup35(Δ2-30)NMG protein formed amyloid lacking Core 1 (Fig.
371 S1-34), but polymerized inefficiently, with only about 15% of this protein being aggregated despite
372 high overproduction from multicopy *GAL1* promoter. In contrast, the Sup35(Δ2-16)NMG protein,
373 overproduced in [*PIN*$^+$] cells, polymerized efficiently, but formed amyloid with shortened Core 1.
374 Finally, the amyloids with 62-144 core produced unstable [*PSI*$^+$], when introduced into yeast cells
375 (24). Thus, it appears likely that such Sup35NM fold rearranges *in vivo* and acquires Core 1. If so, it
376 would be very interesting to find, why some amyloid folds existing *in vitro* are so disfavored *in*
377 *vivo*. The described observations show that the data obtained with Sup35 fibrils spontaneously
378 formed *in vitro* may differ significantly from those obtained with *in vivo* prions.

379

380 **Problems in discrimination of [*PSI*$^+$] variants.** This work revealed some natural problems in
381 discrimination of prion variants within each of the two major [*PSI*$^+$] types. First is that the
382 traditional discrimination based on the nonsense-suppressor phenotype may incorrectly reflect the
383 underlying prion variant, being affected by factors unrelated to Sup35 prion, such as duplication of
384 chromosome I carrying the *ade1-14* gene (34), or [*PIN*$^+$] and [*SWI*$^+$] prions, which, in concert,
385 cause the [*NSI*$^+$] nonsense-suppressor phenotype (35). Such cases were frequent among the tested
386 [*PSI*$^+$] isolates with similar genetic background. S-7 and WS2, S-W8 and W-1112 pairs showed
387 similar colony color, but different nonsense readthrough; S1 and S-7 showed similar readthrough,

bioRxiv preprint doi: https://doi.org/10.1101/604660; this version posted April 10, 2019. The copyright holder for this preprint (which was not certified by peer review) is the author/funder, who has granted bioRxiv a license to display the preprint in perpetuity. It is made available under aCC-BY-NC-ND 4.0 International license.

388 but different colony color; W-VK and W-VL had redder colonies, but higher readthrough than W-
389 1111 and W-1112 (Fig. 3).

390 Another issue is that Cores 2 and 3 can be almost phenotypically silent and/or unstable. This
391 raises the question whether their presence, at least in some cases, should be regarded as a [*PSI*$^+$]
392 variant difference.

393 Some [*PSI*$^+$] variants could be distinguished through different effects of overproduced Sup35
394 (growth retardation in W-L2, antisuppression in W-T7, Fig. 4) or chaperones (14), but it is not
395 certain that many variants can be distinguished in this way. Some of [*PSI*$^+$] isolates obtained in the
396 absence of Btn2, Cur1, Upf1,2,3 and Siw14 proteins, or at reduced activity of Hsp104 are cured by
397 normal levels of these proteins, and thus represent independent variants (reviewed in (36)). Fine
398 details of PK digestion of the region 30-72 could also serve for variants discrimination, but this
399 requires further investigation.

400 Possibly the most universal instrument for discrimination of the [*PSI*$^+$] variants could be testing
401 of their ability to copolymerize with a set of N-terminal Sup35 mutants. This approach allowed to
402 discriminate four variants studied here (15, 16), while the total number of strains, distinguishable in
403 this way, exceeds 20 (C.-Y. King, personal communication). Of note, this approach reflects only the
404 structural differences in Region 1.

405

406 **Details of Sup35 prion structure**. The structures of Sup35 prion cores were analyzed previously
407 by different methods (18, 20, 37), and emerging descriptions differed noticeably, sometimes even
408 within a single study (18). Our data support some earlier findings and contradict others.

409 The most prominent structural feature in our study was the fully protected N-terminal region 2-
410 32. Proline substitution and glycine insertion mutagenesis showed that this region is most critical
411 for [*PSI*$^+$] propagation (15, 16). Remarkably, such alterations, made just three residues away from
412 the N-terminus, interfered with three [*PSI*$^+$] variants of four and, regrettably, closer positions were
413 not tested. The majority of mutations impairing [*PSI*$^+$] propagation also mapped to the same region

bioRxiv preprint doi: https://doi.org/10.1101/604660; this version posted April 10, 2019. The copyright holder for this preprint (which was not certified by peer review) is the author/funder, who has granted bioRxiv a license to display the preprint in perpetuity. It is made available under aCC-BY-NC-ND 4.0 International license.

(38). Finally, the Sup35 region 1-61, fused to GFP, was sufficient to faithfully transmit specific prion fold of variants S-VH, W-VK, W-VL and S-W8, when this fusion protein was seeded by cell lysates and the resulting amyloids were reintroduced to yeast (15, 16).

The 2-32 region of Sup35 amyloids was also the best protected from Hydrogen/Deuterium exchange (20). In contrast, site-specific labeling with fluorescent molecules pyrene maleimide and acrylodan indicated that the region 1-20 is loosely structured and does not form intermolecular contacts (18). The latter result could be an artifact, because fibers were formed from a mix of labeled and unlabeled Sup35 molecules, while prion formation is sensitive to even single residue differences in this region and the dyes used, acrylodan (225Da) and pyrene maleimide (297Da), are twice larger than an average amino acid residue. Summing up the above observations, the region 2-32 represents the key element of Sup35 prion structure for all studied [*PSI*$^{+}$] variants.

The difference in folding of the weak and strong prions was observable as different PK cutting of the region 32-45 (Fig. 2B, S1). Notably, PK cut at the same sites in all preparations, but the proportions were different. PK never cut after Q33, N36, A39, Q40, P41, G43, G44, and this cannot be related to residue specificity of PK, since all these residues, except for P, were good targets for PK at other locations of Sup35NM. Thus, the similarity of cutting sites probably reflects similar local folding of this region. We suggest that the key structural difference of the strong and weak folds is located within the region 2-32 inaccessible for PK. This difference modulates exposure of the region 32-45, causing the difference in accessibility of residues 35, 38, 42 and 45, which allows distinguishing weak and strong folds.

The region 33-72 appears to differ significantly from 2-32 in structure. It was protected from PK only partially, but, furthermore, this protection ceased, when PK cut this region off from the region 2-32. Together with Core 2, such sequence of structures is reminiscent of the structure reported by Krishnan and Lindquist (18), where the regions called Head (20-35) and Tail (about 80-110) are involved in intermolecular contacts, while the intermediate region 35-80, called Central Core, is not. Then, the Head would correspond to the fully protected region 2-32, and the Central

bioRxiv preprint doi: https://doi.org/10.1101/604660; this version posted April 10, 2019. The copyright holder for this preprint (which was not certified by peer review) is the author/funder, who has granted bioRxiv a license to display the preprint in perpetuity. It is made available under aCC-BY-NC-ND 4.0 International license.

Core to the partially protected region and PK -sensitive part of the Region 2, while the Tail coincides very well with our Core 2. Moreover, in strong [*PSI*$^{+}$] Core 2 was shifted about 10 residues towards the N-terminus relatively to "weak" Core 2, and the same shift was observed for the Tail. The only, but significant, difference is that Core 2 was optional, while the Tail was presumed to be of key importance for the prion structure. Of note, the region between the fully protected Core 1 and "weak" Core 2 is mainly formed by oligopeptide repeats (residues 41-97, Fig. 1).

Gorkovskiy and coauthors mapped residues involved in in-register contacts between Sup35 molecules in the region 9-101 (19). According to this work, Tyr-29 is not involved in intermolecular in-register contacts, and is presumed to be in a loop or turn, while Tyr-35 was presumed to form contacts, being in the middle of beta strand. However, in our hands Tyr-29 was not accessible to PK while Tyr-35 was. On the other hand, the finding that Gln-71 forms intermolecular contact, while Tyr-73 does not (19), fits well with the border of the partially protected region at Gln-72.

The "serpentine" model of the Sup35 prion structure proposes that it is composed of short (5-8 residues) beta strands and beta turns alternating in the serpentine manner (39). Our data are poorly compatible with this model. First, because in the serpentine structure all parts of amyloid core are similar in their properties, while we observed asymmetry and fundamental difference of regions 2-32 and 33-72. Second, the N-terminal residues were fully protected from PK, which would be difficult to achieve at the edge of serpentine structure, and suggests that these residues are buried inside of the amyloid structure. Notably, the Rnq1 prion (this work) and fibers of anchorless PrP generated *in vitro* (40) showed a similar property: the terminal region was fully protected from PK, though in these cases it was C-terminus. Third, one can expect from the serpentine structure periodic accessibility to PK corresponding to serpentine turns, which was not observed. Fourth, Core 1 ends at the third of five oligopeptide repeats, while in the serpentine model it is unclear why the remaining two repeats would not realize their similar potential to form amyloid structure.

bioRxiv preprint doi: https://doi.org/10.1101/604660; this version posted April 10, 2019. The copyright holder for this preprint (which was not certified by peer review) is the author/funder, who has granted bioRxiv a license to display the preprint in perpetuity. It is made available under aCC-BY-NC-ND 4.0 International license.

Several observations suggest that Core 1 is larger in weak variants. The region protected from Hydrogen/Deuterium exchange spans residues 1-37 in strong and 1-70 in weak Sup35 fibers (20), which agrees well with much higher fragility of strong fibers (37) and their lower thermal stability (41). In contrast, we observed that the region 33-70 was much better protected from PK in strong [*PSI*$^+$] variants. (Fig. 2, S1). Other observations more consistent with ours are that Gly58Asp (*PNM2*) and Gly54Glu mutations in this region interfere with propagation of strong, but not weak [*PSI*$^+$] variants (42, 43). Thus, despite the obvious discrepancy, these observations do not directly contradict each other, and may be related to different methods of observation.

The *in vitro* obtained "weak" and "strong" Sup35 fibrils showed dramatic difference in fragility (37). Explaining this can be helped by our observation that weak prions usually included Core 2, while strong prions usually lacked it. Due to this, weak fibrils should be wider, while fragility is inversely related to the second power of the width of elongated objects.

The findings described in this work pose some further questions. Why is Core 1 much more important than Cores 2 and 3 *in vivo*, despite their comparable abilities to form amyloid *in vitro*? Why are there just two types of [*PSI*$^+$]? Answering these questions is important for understanding the nature of prions and their interaction with cellular machinery.

Methods

Yeast Strains and Media. Yeast strains used were 74-D694 (*MATa ade1-14 ura3-52 leu2-3,112 his3-Δ200 trp1-289*) and 5V-H19 (*MATa ade2-1 ura3-52 leu2-3,112 SUQ5 can1-100*) and their derivatives harboring different variants of [*PIN*$^+$] and [*PSI*$^+$]. Strains 74-D694 [*PIN*$^+$] (also called OT60 (44)) and 74-D694 [*PIN*$^+$]$_{\text{very high}}$ (45) were used for obtaining new [*PSI*$^+$] variants, and a number of previously selected [*PSI*$^+$] variants of 74-D694 and 5V-H19 strains were also taken for this work (Table 1).

Synthetic complete (SC) media contained 6.7 g/L Yeast Nitrogen Base without amino acids (Difco), 20 g/L glucose or galactose, and required amino acids. For colony color development, SC

bioRxiv preprint doi: https://doi.org/10.1101/604660; this version posted April 10, 2019. The copyright holder for this preprint (which was not certified by peer review) is the author/funder, who has granted bioRxiv a license to display the preprint in perpetuity. It is made available under aCC-BY-NC-ND 4.0 International license.

492 media contained reduced amount of adenine (7mg/l, or 1/3 of standard). Adenine-limiting rich
493 medium (YPDred) contained 5 g/L yeast extract, 20 g/L peptone, 20 g/L glucose and 20 g/L agar.
494
495 **Selection and characterization of [*PSI*$^+$] isolates.** 74-D694 [*psi*$^-$][*PIN*$^+$] cells were transformed
496 with pCM190-SUP35NMG plasmid (46) . Sup35NMG was overproduced for about 24 hours by
497 growing these cells in liquid SC medium lacking doxycycline and uracil, and then cells were
498 streaked on SC plates lacking adenine and supplemented with 20 μg/ml doxycycline. After ~10
499 days of incubation at 30°C, Ade+ clones were picked up, and the presence of [*PSI*$^+$] prion was
500 confirmed by growing cells on YPD_{red} plates with 3mM guanidine-HCl. Isolates S1, WS2, W2 and
501 W3 were obtained in this way, obtaining of other [*PSI*$^+$] isolates is described in the text.
502
503 **[*PSI*$^+$] variants obtained in non-standard ways.** To widen the variety of Sup35 prion structures,
504 we tried to obtain [*PSI*$^+$] in various non-standard ways. The transformants of 74-D694 *Δrnq1* strain
505 with a plasmid pYes2-SUP35NMG were left on SC-Ura glucose plate at 4ºC for about one month.
506 Then white microcolonies appeared on the surface of old red colonies. These white cells had Ade+
507 phenotype sensitive to GuHCl, and thus carried [*PSI*$^+$]. Presumably, when glucose was used up, the
508 plasmid-borne *GAL1-SUP35NMG* gene was derepressed, and Sup35NMG was produced at some
509 intermediate level. This caused [*PSI*$^+$] appearance despite the lack of Rnq1, and the [*PSI*$^+$] cells had
510 a preference in growth due to Ade+ phenotype. All of about 30 such isolates had white colony
511 color, which suggests that they all were of the strong type.
512 Some [*PSI*$^+$] variants were obtained using altered Sup35 as inducer. 29 N-terminal residues
513 from Sup35 of the yeast *Pichia methanolica* (47) were placed ahead of the *S. cerevisiae* Sup35
514 sequence. This protein does not co-aggregate with pre-existing [*PSI*$^+$] (to be published elsewhere),
515 so we expected to obtain a variant with unusual or missing Core 1. Overproduction of this protein
516 caused appearance of [*PSI*$^+$] variants, two of which, S-Pb and W-Pb were analyzed and did not
517 show unusual traits.

bioRxiv preprint doi: https://doi.org/10.1101/604660; this version posted April 10, 2019. The copyright holder for this preprint (which was not certified by peer review) is the author/funder, who has granted bioRxiv a license to display the preprint in perpetuity. It is made available under aCC-BY-NC-ND 4.0 International license.

Two [*PSI*$^+$] isolates were induced by overproduction of Sup35NMG protein with deletion of residues 84-112. This deletion overlaps with Core 2 and was expected to interfere with its appearance. However, both studied variants S-R4b and W-R4b contained Core 2 structures.

Some variants were obtained as non-toxic descendants of lethal or toxic [*PSI*$^+$]. Such [*PSI*$^+$] were obtained in the presence of the centromeric rescue plasmid pRS315 (*LEU2*) carrying *SUP35C* and *SUP45* genes and were unable to lose this plasmid, or lost it very infrequently. The rescue plasmid was lost from the studied descendants. The obtaining and analysis of such [*PSI*$^+$] will be described elsewhere.

Plasmids. Plasmids producing the Sup35NMG protein were based on either pYES2 (Thermo Fisher Scientific) or pCM190 (46) episomal vectors with *URA3* marker. DNA fragment encoding Sup35NMG was inserted between *Bam*HI and *Xba*I sites of pYES2 or into *Bam*HI site of pCM190. The Sup35NMG sequence expressed by these plasmids was: Sup35(1-239)-6*His-Pro-Val-Ala-Thr-eGFP. Integrative variant of this plasmid was obtained by deleting *Nru*I-*Nae*I fragment containing replicator from 2-micron plasmid. Integration was targeted into the *ura3-52* mutant gene. To construct pYES2-SUP35(Δ84-112)NMG plasmid we amplified the *SUP35* region with such deletion from pR1-4 plasmid (28) with primers GAL-Sup35-Df: GGATCGGACTACTAGCAGCTGCCCACTAGCAACAATG and Su35R1: CCTTCTTGGTAGCATTGGC. This DNA fragment was inserted into pYES2-SUP35NMG plasmid cut with PvuII and BalI using quick-fusion cloning kit (no longer produced by Bimake, USA) to replace the related sequence. Production of Sup35NMG and its variants was repressed by glucose and induced by galactose for pYES2-based plasmids, and repressed by 20 mg/l doxycycline or induced by its absence for pCM190- SUP35NMG. pRS315-SUP35C-SUP45 is a centromeric *LEU2* plasmid encoding the Sup35 C domain and Sup45 proteins at native levels.

bioRxiv preprint doi: https://doi.org/10.1101/604660; this version posted April 10, 2019. The copyright holder for this preprint (which was not certified by peer review) is the author/funder, who has granted bioRxiv a license to display the preprint in perpetuity. It is made available under aCC-BY-NC-ND 4.0 International license.

Prion isolation from yeast. [*PSI*$^{+}$] cells were transformed with multicopy plasmids overproducing Sup35NMG under control of *GAL1* promoter. Cells were grown in 150ml of non-inducing synthetic medium to OD600 = 2.5, and then transferred to 300 ml of inducing medium and grown overnight. Preservation of the original prion fold was confirmed by the lack of intracellular fluorescent Sup35NMG rings and by correct colony color of grown cells. Cells were collected to 50 ml Falcon tubes and lysed by vigorous shaking with glass beads in TBS (30 mM Tris-HCl, pH 7.6; 150 mM NaCl) with 5 mM PMSF, 1mM dithiotreitol and 20 µg/ml of RNAse A. The lysate including cell debris was transferred to two 2.3 ml Eppendorf tubes and spun at 20000 g, 4ºC, for 30 min. The pellet was resuspended in TBS with 2 mM PMSF and spun again, resuspended in 1.5 ml of TBS with 2 mM PMSF. Sarcosyl was added to 5%, and the mix was sonicated for 30 (6*5) s at 50% of power of VCX130 sonicator with a 2 mm tip (Sonics and Materials, USA). Lysate was centrifugated at 20000 g, 4ºC, for 3 min. Supernatant (2.7 ml) was loaded to 3.5 ml open-top tube on top of a sucrose gradient made of 250 µl each of 60%, 40% and 20% sucrose. Tubes were spun in an MLS-50 bucket rotor (Beckman Coulter) at 268,000g for 4 hours. Sup35NMG was visually identified by GFP fluorescence in 60% sucrose fraction and collected.

PK digestion and mass spectrometry. Sup35NMG (200 µg/ml) was digested by PK (25ug/ml) in 20 µl for 1 hour at room temperature. PK was inactivated by adding 1 µl of 100 mM PMSF and peptides precipitated by addition of 14 µl of acetone and incubation on ice for 10 min. Peptides were collected by centrifugation at 16000 g for 1 min, dissolved in 20µl of water, precipitated with 30µl acetone, dissolved in 15 µl of water, denatured by boiling for 3 min and analyzed by MALDI-TOF/TOF mass spectrometer UltrafleXtreme (Bruker, Germany). Peptides were identified by MS-MS and/or as groups of related peaks.

Nonsense readthrough measurement. Nonsense readthrough levels were measured for the UGA codon followed by cytidine (UGAc). This extended codon showed the highest readthrough among

bioRxiv preprint doi: https://doi.org/10.1101/604660; this version posted April 10, 2019. The copyright holder for this preprint (which was not certified by peer review) is the author/funder, who has granted bioRxiv a license to display the preprint in perpetuity. It is made available under aCC-BY-NC-ND 4.0 International license.

569 other codons in the S-7 variant of 74-D694 strain (48) and it should not be affected by the *SUQ5*
570 UAA suppressor tRNA of 5V-H19. Yeast cells were transformed with pDB691 plasmid carrying
571 tandem Renilla and firefly luciferase genes separated by the UGAc codon, or with control plasmid
572 pDB690 lacking intermediate nonsense codon (49). The transformants were assayed with the dual
573 luciferase reporter assay system (Promega, USA), using a Glomax 20/20 luminometer (Promega).
574 All assays were repeated three times, and the data are expressed as mean ± SEM.
575
576 **PK resistance index calculation.** To graphically represent the PK resistant structures, we
577 calculated for every residue of Sup35NM the PK resistance index R as a sum of mass spectral peak
578 areas of peptides which include this residue (Fig. 2A and S1). For each preparation, two MALDI
579 spectra were taken, in the reflecton and in the linear mode. The former is more precise and
580 convenient for identification of peptides, but underrepresents heavy peptides. The latter shows more
581 correctly the amount of peptides in the range of 4 to 8 kDa. The peptides in the range of 1 to 4,5
582 kDa were calculated basing on reflecton spectra, for heavier peptides calculation was based on
583 linear spectra with a correction coefficient allowing to merge two datasets by equalizing them at
584 peptides 2-38 (4343,3 Da) or 2-42 (4710,7 Da). The resulting graphs were normalized against their
585 maximum value for each preparation.
586

587 # Acknowledgements

588 We thank Chih-Yen King and Heather True for the kind gift of yeast strains. Mass spectrometry
589 was performed by the Shared-Access Equipment Centre “Industrial Biotechnology” of FRC
590 “Fundamentals of Biotechnology” RAS. The experimental work was primarily funded by the
591 Russian Scientific Foundation grant #17-14-01092 and the Ministry of Science and Higher
592 Education of the Russian Federation. DNA construction was supported by the Russian Foundation
593 for Basic Research grant #17-04-00032.
594

bioRxiv preprint doi: https://doi.org/10.1101/604660; this version posted April 10, 2019. The copyright holder for this preprint (which was not certified by peer review) is the author/funder, who has granted bioRxiv a license to display the preprint in perpetuity. It is made available under aCC-BY-NC-ND 4.0 International license.

References

1. Wickner RB, Edskes HK, Kryndushkin D, McGlinchey R, Bateman D, Kelly A. 2011. Prion diseases of yeast: amyloid structure and biology. Semin Cell Dev Biol 22:469–75.
2. Shewmaker F, Wickner RB, Tycko R. 2006. Amyloid of the prion domain of Sup35p has an in-register parallel beta-sheet structure. Proc Natl Acad Sci U S A 103:19754–19759.
3. Paushkin S V, Kushnirov V V, Smirnov VN, Ter-Avanesyan MD. 1996. Propagation of the yeast prion-like [psi+] determinant is mediated by oligomerization of the SUP35-encoded polypeptide chain release factor. EMBO J 15:3127–34.
4. Pezza JA, Villali J, Sindi SS, Serio TR. 2014. Amyloid-associated activity contributes to the severity and toxicity of a prion phenotype. Nat Commun 5:4384.
5. Ter-Avanesyan MD, Dagkesamanskaya AR, Kushnirov V V, Smirnov VN. 1994. The SUP35 omnipotent suppressor gene is involved in the maintenance of the non-Mendelian determinant [psi+] in the yeast Saccharomyces cerevisiae. Genetics 137:671–676.
6. Ter-Avanesyan MD, Kushnirov V V, Dagkesamanskaya AR, Didichenko SA, Chernoff YO, Inge-Vechtomov SG, Smirnov VN. 1993. Deletion analysis of the SUP35 gene of the yeast Saccharomyces cerevisiae reveals two non-overlapping functional regions in the encoded protein. Mol Microbiol 7:683–92.
7. Helsen CW, Glover JR. 2012. Insight into molecular basis of curing of [PSI +] prion by overexpression of 104-kDa heat shock protein (Hsp104). J Biol Chem 287:542–556.
8. Franzmann TM, Jahnel M, Pozniakovsky A, Mahamid J, Holehouse AS, Nüske E, Richter D, Baumeister W, Grill SW, Pappu R V, Hyman AA, Alberti S. 2018. Phase separation of a yeast prion protein promotes cellular fitness. Science 359.
9. Derkatch IL, Chernoff YO, Kushnirov V V, Inge-Vechtomov SG, Liebman SW. 1996. Genesis and variability of [PSI] prion factors in Saccharomyces cerevisiae. Genetics 144:1375–86.
10. Kushnirov V V, Vishnevskaya AB, Alexandrov IM, Ter-Avanesyan MD. 2007. Prion and

bioRxiv preprint doi: https://doi.org/10.1101/604660; this version posted April 10, 2019. The copyright holder for this preprint (which was not certified by peer review) is the author/funder, who has granted bioRxiv a license to display the preprint in perpetuity. It is made available under aCC-BY-NC-ND 4.0 International license.

621 nonprion amyloids: a comparison inspired by the yeast Sup35 protein. Prion 1:179–184.
622 11. Kushnirov V V, Ter-Avanesyan MD. 1998. Structure and replication of yeast prions. Cell
623 94:13–16.
624 12. Kryndushkin DS, Alexandrov IM, Ter-Avanesyan MD, Kushnirov V V. 2003. Yeast [PSI+]
625 prion aggregates are formed by small Sup35 polymers fragmented by Hsp104. J Biol Chem
626 278:49636–49643.
627 13. Shkundina IS, Kushnirov V V., Tuite MF, Ter-Avanesyan MD. 2006. The role of the N-
628 terminal oligopeptide repeats of the yeast Sup35 prion protein in propagation and
629 transmission of prion variants. Genetics 172:827–835.
630 14. Kushnirov V V, Kryndushkin DS, Boguta M, Smirnov VN, Ter-Avanesyan MD. 2000.
631 Chaperones that cure yeast artificial [PSI+] and their prion-specific effects. Curr Biol
632 10:1443–1446.
633 15. Chang H-Y, Lin J-Y, Lee H-C, Wang H-L, King C-Y. 2008. Strain-specific sequences
634 required for yeast [PSI+] prion propagation. Proc Natl Acad Sci 105:13345–13350.
635 16. Huang YW, Chang YC, Diaz-Avalos R, King CY. 2015. W8, a new Sup35 prion strain,
636 transmits distinctive information with a conserved assembly scheme. Prion 9:207–227.
637 17. Kochneva-pervukhova N V, Chechenova MB, Valouev IA, Kushnirov V V, Smirnov VN,
638 Ter-avanesyan MD. 2001. [PSI +] prion generation in yeast : characterization of the ` strain
639 ' difference. Yeast 489–497.
640 18. Krishnan R, Lindquist SL. 2005. Structural insights into a yeast prion illuminate nucleation
641 and strain diversity. Nature 435:765–72.
642 19. Gorkovskiy A, Thurber KR, Tycko R, Wickner RB. 2014. Locating folds of the in-register
643 parallel -sheet of the Sup35p prion domain infectious amyloid. Proc Natl Acad Sci
644 111:E4615–E4622.
645 20. Toyama BH, Kelly MJS, Gross JD, Weissman JS. 2007. The structural basis of yeast prion
646 strain variants. Nature 449:233–7.

bioRxiv preprint doi: https://doi.org/10.1101/604660; this version posted April 10, 2019. The copyright holder for this preprint (which was not certified by peer review) is the author/funder, who has granted bioRxiv a license to display the preprint in perpetuity. It is made available under aCC-BY-NC-ND 4.0 International license.

21. Tanaka M, Chien P, Naber N, Cooke R, Weissman JS. 2004. Conformational variations in an infectious protein determine prion strain differences. Nature 428:323–8.

22. Keil B. 1992. Specificity of Proteolysis. Springer Berlin Heidelberg, Berlin, Heidelberg.

23. Polevoda B, Sherman F. 2003. N-terminal acetyltransferases and sequence requirements for N-terminal acetylation of eukaryotic proteins. J Mol Biol 325:595–622.

24. Ohhashi Y, Yamaguchi Y, Kurahashi H, Kamatari YO, Sugiyama S, Uluca B, Piechatzek T, Komi Y, Shida T, Müller H, Hanashima S, Heise H, Kuwata K, Tanaka M. 2018. Molecular basis for diversification of yeast prion strain conformation. Proc Natl Acad Sci 115:2389–2394.

25. Vishveshwara N, Bradley ME, Liebman SW. 2009. Sequestration of essential proteins causes prion associated toxicity in yeast. Mol Microbiol 73:1101–14.

26. Zhao X, Rodriguez R, Silberman RE, Ahearn JM, Saidha S, Cummins KC, Eisenberg E, Greene LE. 2017. Heat shock protein 104 (Hsp104)-mediated curing of [PSI+] yeast prions depends on both [PSI+] conformation and the properties of the Hsp104 homologs. J Biol Chem 292:8630–8641.

27. Stansfield I, Jones KM, Kushnirov V V, Dagkesamanskaya AR, Poznyakovski AI, Paushkin S V, Nierras CR, Cox BS, Ter-Avanesyan MD, Tuite MF. 1995. The products of the SUP45 (eRF1) and SUP35 genes interact to mediate translation termination in Saccharomyces cerevisiae. EMBO J 14:4365–4373.

28. Parham SN, Resende CG, Tuite MF. 2001. Oligopeptide repeats in the yeast protein Sup35p stabilize intermolecular prion interactions. EMBO J 20:2111–2119.

29. Valouev I a, Kushnirov V V, Ter-Avanesyan MD. 2002. Yeast polypeptide chain release factors eRF1 and eRF3 are involved in cytoskeleton organization and cell cycle regulation. Cell Motil Cytoskeleton 52:161–73.

30. Sant'Anna R, Fernández MR, Batlle C, Navarro S, de Groot NS, Serpell L, Ventura S. 2016. Characterization of Amyloid Cores in Prion Domains. Sci Rep 6:34274.

bioRxiv preprint doi: https://doi.org/10.1101/604660; this version posted April 10, 2019. The copyright holder for this preprint (which was not certified by peer review) is the author/funder, who has granted bioRxiv a license to display the preprint in perpetuity. It is made available under aCC-BY-NC-ND 4.0 International license.

673 31. Bateman DA, Wickner RB. 2013. The [PSI+] Prion Exists as a Dynamic Cloud of Variants.
674 PLoS Genet 9:1–13.
675 32. Ghosh R, Dong J, Wall J, Frederick KK. 2018. Amyloid fibrils embodying distinctive yeast
676 prion phenotypes exhibit diverse morphologies. FEMS Yeast Res 18.
677 33. McGlinchey RP, Kryndushkin D, Wickner RB. 2011. Suicidal [PSI+] is a lethal yeast prion.
678 Proc Natl Acad Sci 108:5337–5341.
679 34. Chan PHW, Lee L, Kim E, Hui T, Stoynov N, Nassar R, Moksa M, Cameron DM, Hirst M,
680 Gsponer J, Mayor T. 2017. The [PSI+] yeast prion does not wildly affect proteome
681 composition whereas selective pressure exerted on [PSI+] cells can promote aneuploidy. Sci
682 Rep 7:1–15.
683 35. Nizhnikov AA, Ryzhova TA, Volkov K V, Zadorsky SP, Sopova J V, Inge-Vechtomov SG,
684 Galkin AP. 2016. Interaction of Prions Causes Heritable Traits in Saccharomyces cerevisiae.
685 PLoS Genet 12:e1006504.
686 36. Wickner RB, Son M, Edskes HK. 2019. Prion Variants of Yeast are Numerous, Mutable, and
687 Segregate on Growth, Affecting Prion Pathogenesis, Transmission Barriers, and Sensitivity
688 to Anti-Prion Systems. Viruses 11.
689 37. Tanaka M, Collins SR, Toyama BH, Weissman JS. 2006. The physical basis of how prion
690 conformations determine strain phenotypes. Nature 442:585–589.
691 38. Depace AH, Santoso A, Hillner P, Weissman JS. 1998. A Critical Role for Amino-Terminal
692 Glutamine / Asparagine Repeats in the Formation and Propagation of a Yeast Prion. Cell
693 93:1241–1252.
694 39. Kajava A V, Baxa U, Wickner RB, Steven AC. 2004. A model for Ure2p prion filaments and
695 other amyloids: the parallel superpleated beta-structure. Proc Natl Acad Sci U S A
696 101:7885–7890.
697 40. Vázquez-Fernández E, Alonso J, Pastrana MA, Ramos A, Stitz L, Vidal E, Dynin I, Petsch
698 B, Silva CJ, Requena JR. 2012. Structural organization of mammalian prions as probed by

bioRxiv preprint doi: https://doi.org/10.1101/604660; this version posted April 10, 2019. The copyright holder for this preprint (which was not certified by peer review) is the author/funder, who has granted bioRxiv a license to display the preprint in perpetuity. It is made available under aCC-BY-NC-ND 4.0 International license.

limited proteolysis. PLoS One 7:e50111.

41. Alexandrov AI, Polyanskaya AB, Serpionov G V., Ter-Avanesyan MD, Kushnirov V V. 2012. The Effects of Amino Acid Composition of Glutamine-Rich Domains on Amyloid Formation and Fragmentation. PLoS One 7.

42. Derkatch IL, Bradley ME, Zhou P, Liebman SW. 1999. The PNM2 mutation in the prion protein domain of SUP35 has distinct effects on different variants of the [PSI+] prion in yeast. Curr Genet 35:59–67.

43. King CY. 2001. Supporting the structural basis of prion strains: Induction and identification of [PSI] variants. J Mol Biol 307:1247–1260.

44. Bailleul PA, Newnam GP, Steenbergen JN, Chernoff YO. 1999. Genetic Study of Interactions Between the Cytoskeletal Assembly Protein Sla1. Genetics 153:81–94.

45. Bradley ME, Edskes HK, Hong JY, Wickner RB, Liebman SW. 2002. Interactions among prions and prion "strains" in yeast. Proc Natl Acad Sci U S A 99 Suppl 4:16392–16399.

46. Gari E, Piedrafita L, Aldea M, Herrero E. 1997. A set of vectors with a tetracycline-regulatable promoter system for modulating gene expression inSaccharomyces cerevisiae. Yeast 13:837–848.

47. Kushnirov V V, Ter-Avanesyan MD, Didichenko SA, Smirnov VN, Chernoff YO, Derkach IL, Novikova ON, Inge-Vechtomov SG, Neistat MA, Tolstorukov II. 1990. Divergence and conservation of SUP2 (SUP35) gene of yeast Pichia pinus and Saccharomyces cerevisiae. Yeast 6:461–472.

48. Urakov VN, Mitkevich O V, Safenkova I V, Ter-Avanesyan MD. 2017. Ribosome-bound Pub1 modulates stop codon decoding during translation termination in yeast. FEBS J 284:1914–1930.

49. Keeling KM, Lanier J, Du M, Salas-Marco J, Gao L, Kaenjak-Angeletti A, Bedwell DM. 2004. Leaky termination at premature stop codons antagonizes nonsense-mediated mRNA decay in S. cerevisiae. RNA 10:691–703.

bioRxiv preprint doi: https://doi.org/10.1101/604660; this version posted April 10, 2019. The copyright holder for this preprint (which was not certified by peer review) is the author/funder, who has granted bioRxiv a license to display the preprint in perpetuity. It is made available under aCC-BY-NC-ND 4.0 International license.

725 50. Dagkesamanskaya AR, Ter-Avanesyan MD. 1991. Interaction of the yeast omnipotent
726 suppressors SUP1(SUP45) and SUP2(SUP35) with non-mendelian factors. Genetics
727 128:513–20.

728

729

bioRxiv preprint doi: https://doi.org/10.1101/604660; this version posted April 10, 2019. The copyright holder for this preprint (which was not certified by peer review) is the author/funder, who has granted bioRxiv a license to display the preprint in perpetuity. It is made available under aCC-BY-NC-ND 4.0 International license.

730 # Figure legends

731 **Fig. 1.** PK-resistant regions of Sup35 prions. A superposition of Sup35 peptides identified after PK
732 digestion of Sup35NMG preparations from all [*PSI*$^+$] isolates. The peptides were divided into six
733 groups according to their start and end positions. Graph shows the number of identified peptides in
734 each group, which include a given amino acid residue. In other words, the graph was obtained by
735 placing identified peptides in accordance with their coordinates one above the other with a height of
736 1. Peptides of the groups 2S and 2W were found more often in Cores 2 of strong and weak [*PSI*+]
737 variants, respectively. Peptides of the 2-3 group of fragments were observed in variants S-L20 and
738 S-T9 at low abundance. Note that the large variation in the abundance and the frequency of
739 appearance of the peptides is not reflected here.
740
741 **Fig. 2.** Structural analysis of selected [*PSI*$^+$] variants. (*A*) PK resistance index for the Sup35 region
742 2-222 of variants L20, S-W8-R4 and W-1112, calculated as described in the text. In contrast to Fig.
743 1, the contribution of each peptide was proportional to its MS peak area. (*B*) MALDI-TOF spectra
744 (linear mode) of PK digests of Sup35-NMG of S-VH, S-W8, W-VK and W-VL variants. All
745 peptides in this mass range in these spectra belong to Core 1 and start from Ser2, so only the
746 number of their C-terminal residue is given below each spectrum. The variants in panel A were
747 selected to represent the diversity of Core2 and Core 3 structures. Panel B show different types of
748 Core 1 on an example of a well characterized set of variants (15, 16). Other variants are presented in
749 Fig. S1.
750
751 **Fig. 3. Suppressor phenotypes of [*PSI*$^+$] variants.** (*A*) Indicated variants were spotted to YPD-red
752 plate and grown for 4 days. (*B*) Readthrough of the nonsense codon UGAc. Standard error is
753 indicated.
754

bioRxiv preprint doi: https://doi.org/10.1101/604660; this version posted April 10, 2019. The copyright holder for this preprint (which was not certified by peer review) is the author/funder, who has granted bioRxiv a license to display the preprint in perpetuity. It is made available under aCC-BY-NC-ND 4.0 International license.

Fig. 4. Strong and weak [*PSI+*] variants differ by the effects of overproduction of Sup35 and Hsp104. The indicated [*PSI+*] variants of 74-D694 and 5V-H19 strains were transformed with the multicopy plasmids based on YEplac181 (*LEU2*) carrying the *HSP104*, *SUP35* and *SUP35NM* genes as indicated. Also, the "cen*SUP35*" panel used the centromeric pRS315-SUP35 *LEU2* plasmid and the "multi *SUP35*+*SUP45*" panels used multicopy YEplac195 *URA3* plasmid with *SUP35* and *SUP45* genes. SC media contained reduced amount of adenine for colony color development. Photographs were taken on the fourth day after transformation.

Fig. 5. Manipulations with Core 2. Left: the schemes of experiments. Straight lines show amyloid Cores 1 and 2, wavy line: presumably unstructured regions, pink line: two added oligopeptide repeats (9+10 residues). Right: Sup35NM PK resistance profiles before (blue line) and after experiments. (A) Attempted Core 2 elimination by overproduction of Sup35(Δ84-112)NMG with deletion covering a larger part of Core 2. (B) Core 2 was not eliminated when 2 repeats were added between Cores 1 and 2.

bioRxiv preprint doi: https://doi.org/10.1101/604660; this version posted April 10, 2019. The copyright holder for this preprint (which was not certified by peer review) is the author/funder, who has granted bioRxiv a license to display the preprint in perpetuity. It is made available under aCC-BY-NC-ND 4.0 International license.

Table 1. The yeast strains and [*PSI*$^+$] variants used

Variant	Original name/comment	Source/Reference
	Yeast strain 74-D694	
[*psi*-][*PIN*+]	OT60, parent for non-toxic [*PSI*$^+$] obtained in this work	(44) Y. Chernoff
[*psi*-][*PIN*$^+$]$_{\text{very high}}$	Parent for the lethal and toxic isolates	(45) S. Liebman
WS2		This work
W2		This work
W3		This work
W-L2		This work
W-Pb		This work
W-T7		This work
W-R4		This work
S-7	7-74-D694, also known as OT56*	(44) Y. Chernoff
S1		This work
S1-R4		This work
S-L4		This work
S-L6		This work
S-L20		This work
S-Pb		This work
S-R4b		This work
S-Cl1		This work
S-Cl2		This work
W-HT2889	Heather True collection #2889	H. True
	Yeast strain 5V-H19	
S-VH0†	Our collection; [*PSI*$^+$] originates from Albert Hinnen strain AH216	(50)
S-1109	Our collection #1109	
W-1111	Our collection #1111	
W-1112	Our collection #1112	
S-VH†	VH	(15) C.Y. King
S-W8	W8	(16) C.Y. King
W-VK	VK	(15) C.Y. King
W-VL	VL	(15) C.Y. King

The [*PSI*$^+$] variants were named so that the first letter indicates the [*PSI*$^+$] type, as defined in this work. S: strong, W: weak, L: lethal, T: toxic. A letter was added to established names VH, W8, VK and VL to avoid confusions, e.g. W8 is strong, rather than weak. *7-74-D694 and OT56 are strain names, rather than names of a prion variant. †S-VH0 and S-VH are the same [*PSI*$^+$] isolate, but they were separated to different labs for 20 years and [*PIN*$^+$] was selectively cured with guanidine hydrochloride in S-VH (43).

bioRxiv preprint doi: https://doi.org/10.1101/604660; this version posted April 10, 2019. The copyright holder for this preprint (which was not certified by peer review) is the author/funder, who has granted bioRxiv a license to display the preprint in perpetuity. It is made available under aCC-BY-NC-ND 4.0 International license.

779 **Table 2. Location of Sup35 Cores 2 and 3.**

	Weak [*PSI*$^+$]			Strong [*PSI*$^+$]	
Name	Core 2	Core 3	Name	Core 2	Core 3
WS2	96, 101 - 120*	-	S-7	91 - 104	-
W2	-	-	S-7-3	81 - 100*	125 - 148
W3	91 - 120	-	S-7-4	82,92 - 100,113*	-
W-L2	(91,96,101) - 123	133 - 153*	S1	82 - 100, 92 - 113	-
W-T7	81 - 100, 92 - 120	133-149	S1-R4	72, 82 - 100*	-
W-Pb	91 - 121	-	S-L4	72, 82 - 100*	-
W-R4b	(92, 96) - (104, 113, 121)	133 - 148	S-L6	-	-
W-HT2889	91 - 122	-	S-L20	82 - 100	91 - 144*†
W-1111	91, 96 - 120	-	S-Pb	92 - 115	-
W-1112	91 - 121	-	S-R4b	91 - 113	-
W-1112-R14a, R14b	91 - 121	-	S-Cl1	82, 92 - 100, 113*	-
W-VK	96 - (113, 120)	-	S-Cl2	-	-
W-VL	-	-	S-VH0	-	125 - 148
			S-1109	82 - 100*	-
	Amyloid		S-VH	82 - 100	-
Δ2-30	81 - 113	-	S-W8	91 - (104, 113)	-
			S-W8-R14a	91 - 121	(125, 133) -148
			S-W8-R14b	91 - 121	-

780 The borders of the Cores were defined as the biggest increment or decrement of the PK resistance
781 index R per three sequential residues. In cases of nearly equal maximal increments or decrements
782 two or three values are given for borders. *Index R is below 0.1. †Core 2-3.

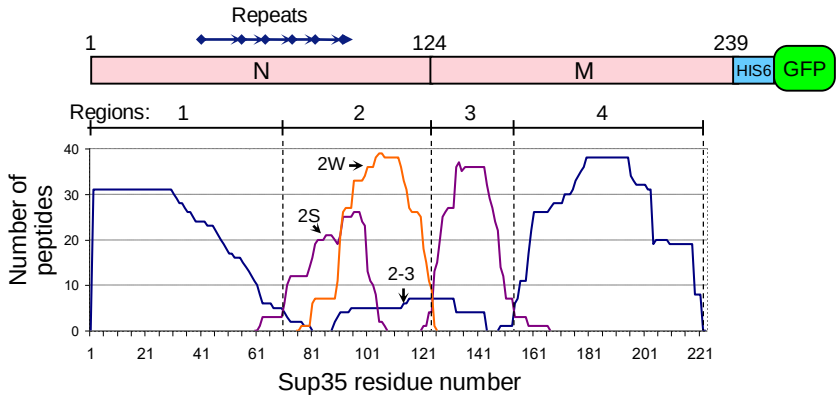
Repeats
1
124
239
N
M
HIS6
GFP
Regions:
1
2
3
4
2W
2S
2-3
Number of peptides
0
10
20
30
40
1
21
41
61
81
101
121
141
161
181
201
221
Sup35 residue number

Figure 1

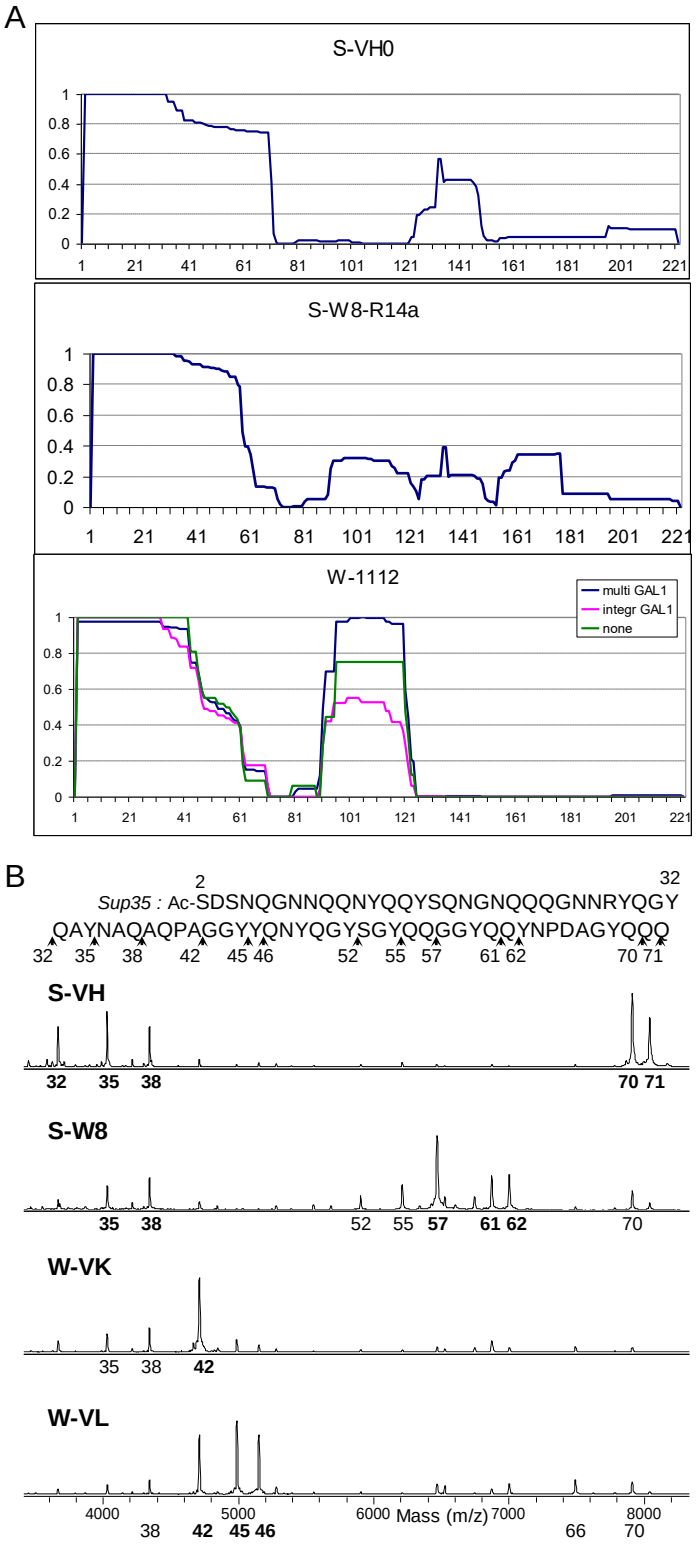
A
S-VH0
S-W8-R14a
W-1112
multi GAL1
integr GAL1
none
B
2
32
Sup35 : Ac-SDSNQGNNQQNYQQYSQNGNQQQGNNRYQGY
QAYNAQAQPAGGYYQNYQGYSGYQQGGYQQYNPDAGYQQQ
S-VH
S-W8
W-VK
W-VL
Mass (m/z)

Figure 2

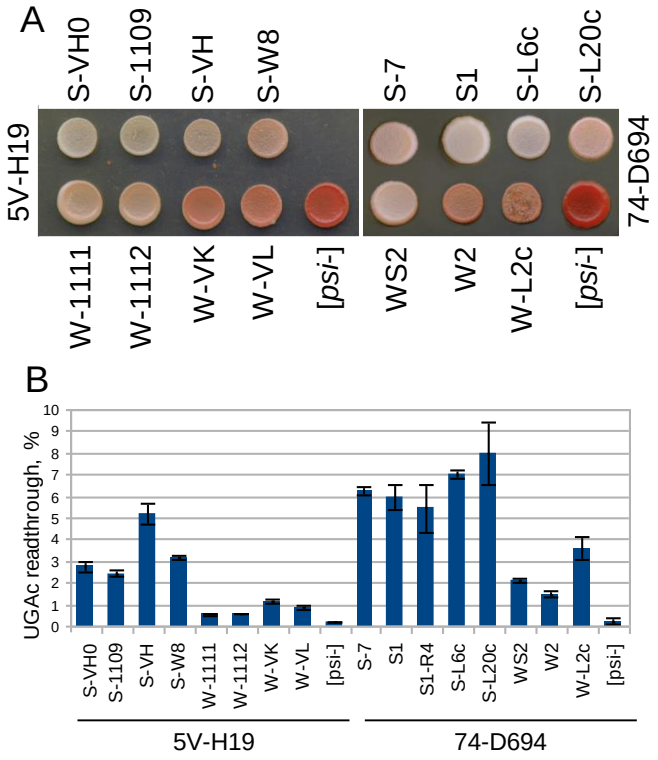
A
S-VH0
S-1109
S-VH
S-W8
S-7
S1
S-L6c
S-L20c
5V-H19
74-D694
W-1111
W-1112
W-VK
W-VL
[psi-]
WS2
W2
W-L2c
[psi-]
B
UGAc readthrough, %
0
1
2
3
4
5
6
7
8
9
10
S-VH0
S-1109
S-VH
S-W8
W-1111
W-1112
W-VK
W-VL
[psi-]
S-7
S1
S1-R4
S-L6c
S-L20c
WS2
W2
W-L2c
[psi-]
5V-H19
74-D694

Figure 3

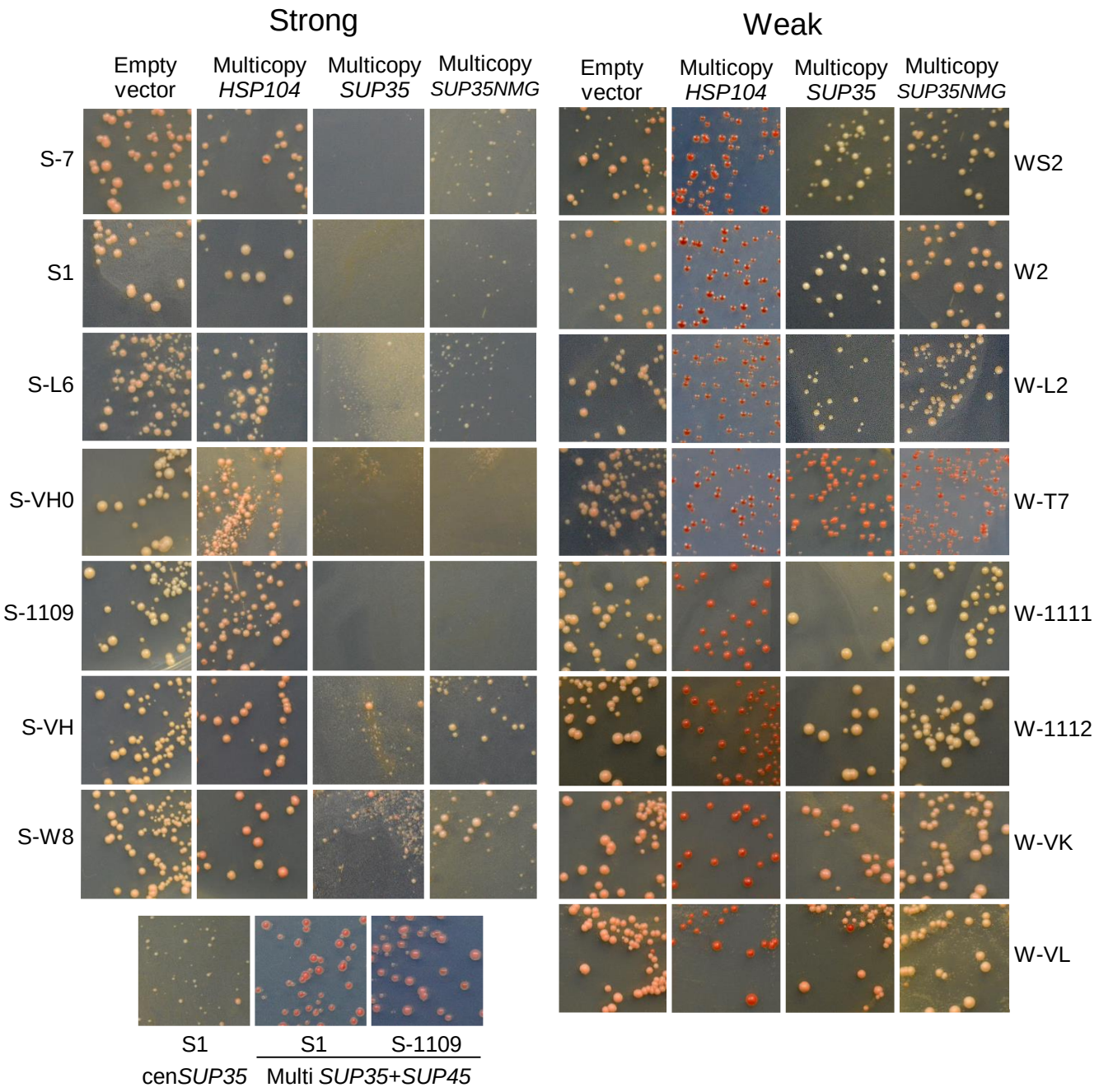
Strong
Weak
Empty vector
Multicopy HSP104
Multicopy SUP35
Multicopy SUP35NMG
S-7
S1
S-L6
S-VH0
S-1109
S-VH
S-W8
WS2
W2
W-L2
W-T7
W-1111
W-1112
W-VK
W-VL
S1
cenSUP35
S1
S-1109
Multi SUP35+SUP45

Figure 4

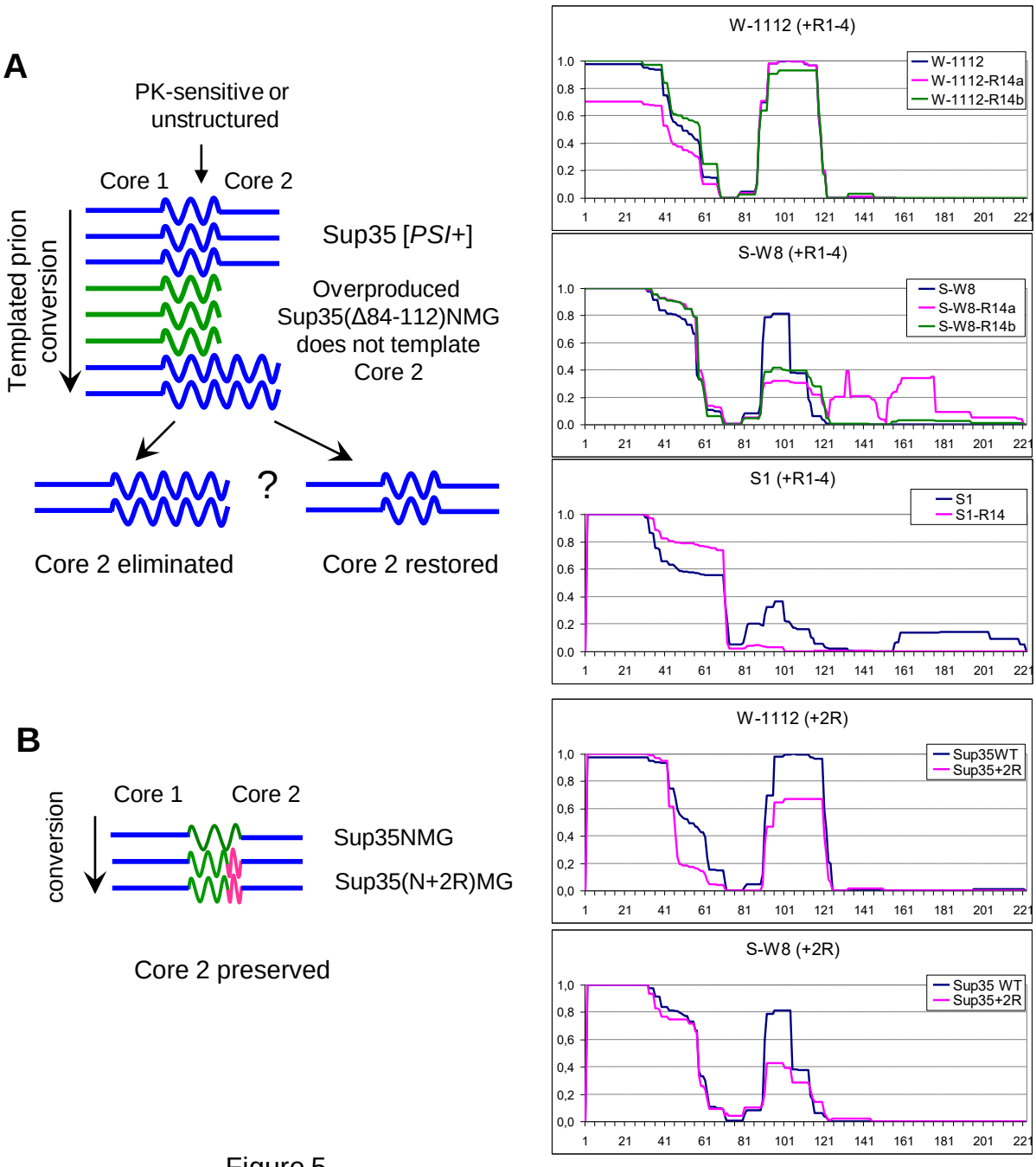
A
PK-sensitive or
unstructured
Core 1
Core 2
Templated prion
conversion
Sup35 [PSI+]
Overproduced
Sup35(Δ84-112)NMG
does not template
Core 2
?
Core 2 eliminated
Core 2 restored
B
conversion
Core 1
Core 2
Sup35NMG
Sup35(N+2R)MG
Core 2 preserved
W-1112 (+R1-4)
W-1112
W-1112-R14a
W-1112-R14b
S-W8 (+R1-4)
S-W8
S-W8-R14a
S-W8-R14b
S1 (+R1-4)
S1
S1-R14
W-1112 (+2R)
Sup35WT
Sup35+2R
S-W8 (+2R)
Sup35 WT
Sup35+2R

Figure 5